PHYSICAL REVIEW B **87**, 201202(R) (2013)

Electric field ionization of gallium acceptors in germanium induced by single-cycle terahertz pulses

Y. Mukai,[1] H. Hirori,[2,*] and K. Tanaka[1,2,†]

[1]*Department of Physics, Graduate School of Science, Kyoto University, Sakyo-ku, Kyoto 606-8502, Japan*

[2]*Institute for Integrated Cell-Material Sciences (WPI-iCeMS), Kyoto University, and JST-CREST, Kyoto 606-8501, Japan*

(Received 24 January 2013; revised manuscript received 2 May 2013; published 20 May 2013)

The electric field ionization of gallium acceptors in germanium was studied by using terahertz-pump–terahertz-probe spectroscopy. As the pump electric field increases, the distinct absorptions due to acceptor transitions centered at 2.0 and 2.2 THz decrease, and simultaneously, a free carrier response emerges in the lower frequency region. These behaviors clearly show that the terahertz-pump pulse ionizes neutral acceptors. The pump electric field dependence of the released hole density is reproduced by a model assuming direct field-assisted tunneling of acceptors.

DOI: 10.1103/PhysRevB.87.201202 PACS number(s): 78.40.Fy, 42.65.Re, 71.55.Ak, 78.47.J−

The interactions of impurity states in semiconductors with terahertz (THz) electromagnetic waves have attracted considerable attention because of their importance in fundamental physics and technological applications. Shallow impurities have a set of discrete electronic bound states similar to the Rydberg series of the free hydrogen atom. The excitation energies between these states lie in the few meV or THz spectral region.[1] The ability to induce nonlinear interactions of impurity states with high-power THz pulses has opened up the possibility of coherent manipulation of quantum bits in ubiquitous semiconductors.[2,3]

For ultrafast coherent manipulation of impurity states, the duration of the controlling THz pulse should be shorter than the coherence time.[4] Moreover, in order to keep the pulse area large enough to induce a population inversion, the peak electric field of the controlling pulse must be intense. In the high electric field regime, the nonlinear process of ionizing impurities through THz-pulse irradiation is crucial for coherent manipulation. So far, ionization phenomena such as multiphoton ionization in shallow impurity states and phonon-assisted tunneling in deep impurity states have been studied in the weak electric field regime by means of nanosecond far-infrared laser pulse irradiation.[5,6] To be able to study the high electric field regime, the nonlinear process of ionizing impurities with THz pulse irradiation is crucial for coherent manipulation. The recent development of ultraintense THz laser systems generating phase-stable transients has enabled us to study coherent THz manipulation[7–9] and fascinating THz nonlinear phenomena in various materials.[10–12] It is claimed that the field ionization process may play a key role in these nonlinear phenomena. However, the ionization process under instantaneous high electric fields is not well understood.

In this Rapid Communication, we report on the nonlinear field ionization process of gallium acceptors in germanium (Ge:Ga) studied by using THz-pump–THz-probe spectroscopy. As the THz-pump electric field increases, the absorption peaks corresponding to the internal acceptor transitions centered at 2.0 and 2.2 THz disappear and a free carrier response appears in the lower frequency region. An analysis of these data based on the Drude-Lorenz model revealed that the THz-pump pulse ionizes the neutral acceptors and releases holes from the acceptors. The dependence of the released free hole density on the pump electric field is in good agreement with a theoretical calculation assuming a direct field-assisted tunneling process.

Figure 1 shows the experimental setup of the THz-pump–THz-probe measurement. THz pulses were generated by optical rectification of femtosecond laser pulses in a $LiNbO_3$ crystal by using the tilted-pump-pulse-front scheme.[13–15] An amplified Ti:sapphire laser (repetition rate 1 kHz, central wavelength 780 nm, pulse duration 100 fs, and 4 mJ/pulse) was used as the light source. As shown in the inset of Fig. 1, the generated THz pulse was split into pump and probe pulses on the same axis by means of internal reflection between a pair of wire-grid polarizers (WG1 and WG2). The ratio between the pump and probe electric fields is determined by the relative angle θ between the polarization axes of WG1 and WG2 and is given by $1 : \sin^2\theta$, where the polarization axis of WG2 is parallel to the THz electric field. The delay between two pulses of 200 ps corresponds to the round-trip time between two wire-grid polarizers (WG1 and WG2), allowing us to neglect the effect of the pump electric field on the spectra observed by the probe pulse. The other pair of wire-grid polarizers (WG3 and WG4) was used to change the field amplitudes of the pump and probe pulses without modifying their wave forms or polarization directions. In addition, in all the experiments, the electric fields of the probe pulses were kept sufficiently below 1 kV/cm, enabling us to rule out spectral modulation due to the probe pulse incidence.[16–18] The sample of gallium-doped germanium (Ge:Ga) crystal [Czochralski method, thickness of 500 μm, room temperature resistivity of 3.6($\pm$0.9) Ω cm, and nominal impurity density of 1.2×10^{15} ($\pm$0.3) cm^{-3}] was mounted in vacuum on a liquid-helium-cooled cold finger and cooled to 10 K. The temperature was measured with a thermocouple. The polarizations of the pump and probe pulses were the same and along the $\langle 110 \rangle$ direction of the sample.

The electro-optic (EO) sampling technique with a 1-mm-thick ZnTe crystal was used to detect the electric field of the pump and probe pulses transmitted through the sample. Figure 2(a) shows a typical THz input pulse incident upon the sample and the output pulse after propagation through the sample, and Fig. 2(b) shows their intensity spectra. The relative amplitudes and phases of the Fourier components can be obtained from the measured electric fields of the pulses shown in Fig. 2(a). Hence, the complex dielectric constant (or

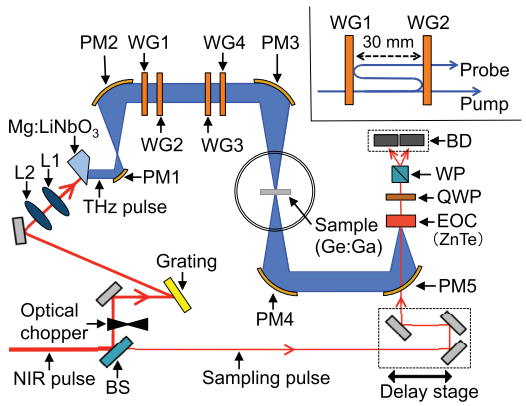

FIG. 1. (Color online) (a) Schematic configuration of THz-pump–THz-probe spectroscopy. L: lens; BS: beam splitter; PM: off-axis parabolic mirror; WG: wire-grid polarizer; EOC: electro-optic crystal; BD: balanced detector; QWP: quarter wave plate; and WP: Wollaston prism. The configuration of the setup for THz generation is the same as in Ref. 15. The inset shows that the THz pulse is split into two pulses using partial reflection between WG1 and WG2. The pulse intensity is tuned by the rotation of WG3. The distances between wire grids are 30 mm (WG1 and WG2), 50 mm (WG2 and WG3), and 40 mm (WG3 and WG4), respectively.

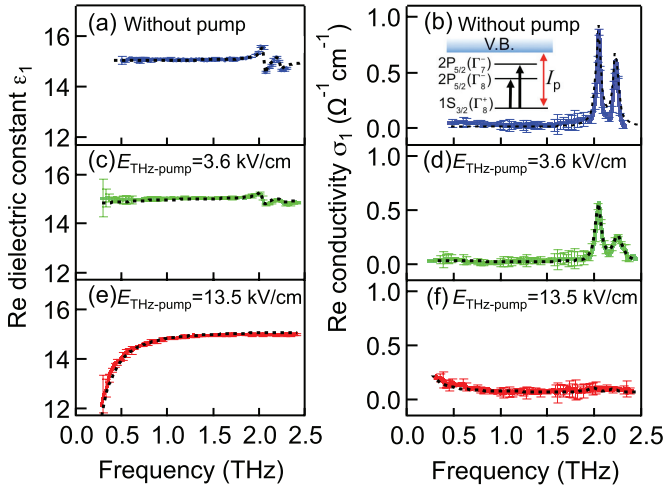

FIG. 3. (Color online) Real part of the dielectric constant and conductivity of Ge:Ga at 15 K for different THz electric fields: (a), (b) without pump excitation; (c), (d) $E_{\text{THz-pump}} = 3.6$ kV/cm; (e), (f) $E_{\text{THz-pump}} = 13.5$ kV/cm. Dashed lines show fitting curves with the Drude-Lorentz model described by Eq. (1). The inset shows the primary excitation paths between the acceptor levels.

conductivity) can be completely characterized by measuring the THz pulse traces with and without samples.[19]

The panels of Fig. 3 show the real part of the dielectric constant ε_1 and conductivity σ_1 after THz-pump pulse excitations. In particular, Fig. 3(b) shows the real part of the conductivity σ_1 obtained by THz time-domain spectroscopy without a pump excitation. Here, the spectral analysis was conducted in the 0.3–2.4 THz range. The absorption peaks at 2.0 and 2.2 THz are internal acceptor transitions of $1S_{3/2}(\Gamma_8^+) \rightarrow 2P_{5/2}(\Gamma_8^-)$ and $1S_{3/2}(\Gamma_8^+) \rightarrow 2P_{5/2}(\Gamma_7^-)$, respectively.[20,21] The maximum peak field of the pump pulse used in this experiment was estimated to be 13.5 kV/cm inside the sample by calibrating the EO sampling signal in a way that took account of Fresnel loss.[22] As shown in the figures, as the pump electric field increases, the conductivity around 2 THz, i.e., the acceptor absorption, decreases and eventually vanishes. Below 1 THz, the conductivity increases, and at the same time, the real part of the dielectric constant decreases, implying the emergence of a free carrier response.

The phenomenological Drude-Lorentz model is able to reproduce the obtained spectra. According to this model,

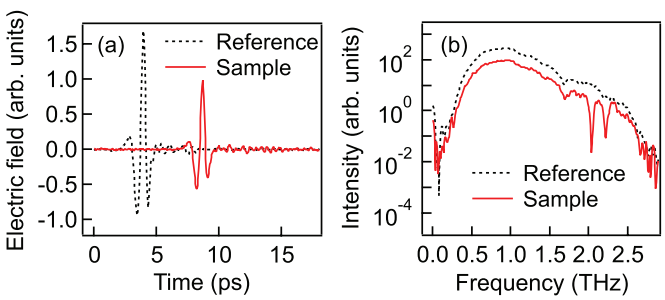

FIG. 2. (Color online) (a) THz field temporal profiles and (b) power spectra with and without (reference) the sample at 15 K.

the complex dielectric constant $\tilde{\varepsilon}(\omega) = \varepsilon_1(\omega) + i\sigma_1(\omega)/\varepsilon_0\omega$ is given by

$$\tilde{\varepsilon}(\omega) = \varepsilon_b + \frac{\omega_p^2}{-\omega^2 - i\omega\gamma} + \frac{e^2 N_b \Gamma_1}{m_0 \varepsilon_0} \sum_j \frac{f_j}{\omega_j^2 - \omega^2 - i\omega\gamma_j}, \quad (1)$$

where ω is angular frequency, e is the elementary charge, m_0 is the mass of the free electron, and $\varepsilon_b = 15.3$ is the background dielectric constant of germanium.[23] The second term is the Drude dispersion that characterizes the free carrier response in terms of the carrier scattering rate γ and the plasma frequency $\omega_p = \sqrt{N_f e^2/m_{hh}^* \varepsilon_0}$, with the free hole density N_f, the effective mass of the heavy hole $m_{hh}^* = 0.35 m_0$,[24] and the vacuum permittivity ε_0. The third term is the Lorentz dispersion that represents the internal transitions between the acceptor levels, and it is characterized by ω_j, f_j, and γ_j, which are, respectively, the resonant frequency, oscillator strength, and damping constant of the jth Lorentz oscillator. Notice that j (=1 and 2) corresponds to the two acceptor transitions of $1S_{3/2}(\Gamma_8^+) \rightarrow 2P_{5/2}(\Gamma_8^-)$ and $1S_{3/2}(\Gamma_8^+) \rightarrow 2P_{5/2}(\Gamma_7^-)$ shown in the inset of Fig. 3(b). The oscillator strengths f_1 and f_2 are given as 0.046 and 0.033, respectively.[23] N_b is the bound hole density, and $\Gamma_1 = 13.36$ is the Luttinger valence band parameter.[23,25,26] The determination of the absorption linewidth ($\gamma_1/2\pi = 0.03$ THz) for the no-THz-pump case is limited by the system's resolution ($\gamma_{sys}/2\pi \sim 0.02$ THz). A simple deconvolution, $\sqrt{(\gamma_1/2\pi)^2 - (\gamma_{sys}/2\pi)^2}$, gives a larger value (0.02 THz) than in the literature (0.012 THz).[27]

The dashed lines in Fig. 3 are theoretical curves obtained by least-squares fitting of the experimental data curves to Eq. (1) using N_b, ω_j, and γ_j as fitting parameters. The fitted value N_b ($=N_b^0$) for the no-THz-pump case shown in Figs. 3(a) and 3(b)

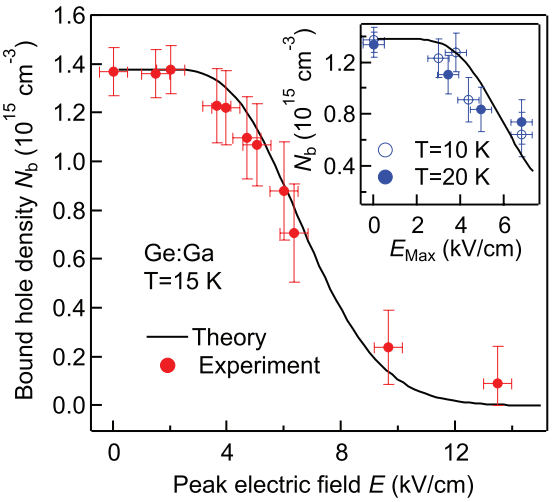

FIG. 4. (Color online) Bound hole density after the THz-pump pulse irradiation at 15 K. The symbols show experimental values deduced by fitting the optical constant (Fig. 3). The solid line is the theoretical calculation assuming the direct field-assisted tunneling process described by Eqs. (2)–(4). The inset shows the data measured at $T = 10$ and 20 K.

is deduced to be $\sim 1.4 \times 10^{15}$ cm^{-3} and is comparable to the acceptor concentration obtained from the electric resistivity measurement. (The uncertainties are typically $\pm 20\%$, owing mainly to excessive attenuation caused by the sample being too thick for the weak higher frequency components above 1.5 THz and the error in the multiparameter fitting.) In addition, the fitted value of $N_f \sim 1.3 \times 10^{15}$ cm^{-3} for the maximum electric field case in Figs. 3(e) and 3(f) is in good agreement with N_b^0 obtained for the no-THz-pump case.[28] These results suggest that the incident THz pulses ionize the acceptor impurities, and the free holes released from the acceptors contribute to the free carrier response described by the Drude dispersion.

Figure 4 shows the THz-pump electric field dependence of the estimated bound hole density N_b. The bound hole density decreases with increasing electric field. The field dependence shows that the acceptor ionization starts from around 5 kV/cm, and the acceptors are completely ionized above 10 kV/cm. This value of the electric field is comparable to the static electric field necessary to ionize gallium acceptors, which is estimated as $E_p = I_p/ea_B^* \approx 10$ kV/cm (binding energy $I_p = 11.3$ meV and effective Bohr radius $a_B^* \approx 10$ nm).[1,29] Thus, the THz field induces a remarkable distortion of the Coulomb potential between the hole and the gallium ion, causing the bound hole to tunnel through the lowered potential barrier.

In order to treat tunneling ionization in a strong THz electric field, it is necessary to solve the time-dependent Schrödinger equation. The Keldysh parameter K,[30] an indicator that distinguishes between the perturbative multiphoton ($K \gg 1$) and quasistatic tunneling regimes ($K \ll 1$), becomes unity when the applied electric field strength and frequency are 4.6 kV/cm and 1 THz.[31] However, in the high field regime where the ionization rate is large, we may use the adiabatic approximation and assume that the released hole density can be estimated from a rate equation with a static field-assisted tunneling time. Moreover, since the 200-ps delay between pump and probe pulses is much shorter than the recombination time in Ge:Ga, i.e., $\tau_b \sim 6$ ns,[32–35] the recombination process of free holes with ionized acceptors can be neglected. The time evolution of the bound hole density under THz pulse irradiation can thus be described by

$$\frac{dN_b(t)}{dt} = -\tau_t^{-1}(t)N_b(t), \tag{2}$$

where $\tau_t(t)$ is the direct tunneling time from the acceptor state to the valence band. In the case of acceptors in semiconductors, the tunneling rate is given by[36,37]

$$\tau_t^{-1}(t) = \omega_0 \left(\frac{6\alpha}{E_{\text{THz-pump}}(t)} \right)^{2n_1^*-1} \exp\left(-\frac{\alpha}{E_{\text{THz-pump}}(t)} \right), \tag{3}$$

where the following parameters defined in Ref. 37 are used for the gallium acceptor in germanium: $\omega_0 = 6.7 \times 10^{13}$ s^{-1}, $n_1^* = 0.47$, and $\alpha = 16$ kV/cm. From Eq. (3), the tunneling time can be estimated to be ~ 0.5 ps at an electric field of 5 kV/cm. We can exclude the effect of photoexcitation of holes from the ground state to the excited Rydberg states as the dominant cause of the ionization process because the number of photons in the pump THz-pulse source between 2.0 and 2.3 THz ($\sim 10^9$ photons) is about 100 times smaller than the number of impurities in the excited volume ($\sim 2 \times 10^{11}$ atoms).

By integrating Eq. (2), the remaining bound hole density can be represented as follows:

$$N_b^{\text{cal}} = N_b^0 - \int_0^\infty \tau_t^{-1}(t)N_b(t)dt. \tag{4}$$

Using the temporal profile of the pump electric field $E_{\text{THz-pump}}(t)$ in Fig. 2(a), we can numerically calculate the bound hole density N_b^{cal} from Eq. (4) without any fitting parameters. In Fig. 4, the theoretical curve obtained from Eqs. (3) and (4) reproduces the experimental values over the whole range of electric field strengths. This result means that the direct field-assisted tunneling process dominates the ionization of acceptors. As shown in the inset of Fig. 4, the field dependence of the bound hole density is not sensitive to the temperature difference. These results indicate that in the high field regime, the phonon-assisted tunneling process negligibly contributes to the shallow impurity ionization, despite that it has been shown that the phonon-assisted tunneling process plays an important role in impurity ionization in the weaker electric field regime, i.e., below one tenth of E_p.[5]

In summary, we have investigated the electric field dependence of the THz optical constant of gallium-doped germanium by using THz-pump–THz-probe spectroscopy. As the peak electric field strength of the THz pump increases, the absorption peaks due to the internal acceptor levels disappear and the Drude dispersion appears in the THz frequency region. Good agreement between the experimental results and theoretical calculations assuming a direct field-assisted tunneling

process implies that the interaction between impurities and THz field enters the adiabatic direct tunneling regime.

We would like to thank Masaya Nagai for his help in the initial stage of this work and Susumu Komiyama for stimulating discussions. This study was supported by KAKENHI (Grants No. 24760042, No. 23244065, and No. 20104007) from the Japan Society for the Promotion of Science (JSPS) and the Ministry of Education, Culture, Sports, Science, and Technology (MEXT) of Japan and by a Grant-in-Aid from the Global COE Program, "The Next Generation of Physics, Spun from Universality and Emergence," of MEXT.

*hirori@icems.kyoto-u.ac.jp
†kochan@scphys.kyoto-u.ac.jp

[1] P. Y. Yu and M. Cardona, *Fundamentals of Semiconductors; Physics and Materials Properties* (Springer, Berlin, 2010).
[2] B. E. Cole, J. B. Williams, B. T. King, M. S. Sherwin, and C. R. Stanley, Nature (London) **410**, 60 (2001).
[3] P. T. Greenland, S. A. Lynch, A. F. G. van der Meer, B. N. Murdin, C. R. Pidgeon, B. Redlich, N. Q. Vinh, and G. Aeppli, Nature (London) **465**, 1057 (2010).
[4] L. Allen and J. H. Eberly, *Optical Resonance and Two-Level Atoms* (Dover, New York, 1987).
[5] S. D. Ganichev and W. Prettl, *Intense Terahertz Excitation of Semiconductors* (Oxford University Press, New York, 2006).
[6] M. Leung and H. D. Drew, Appl. Phys. Lett. **45**, 675 (1984).
[7] C. W. Luo, K. Reimann, M. Woerner, T. Elsaesser, R. Hey, and K. H. Ploog, Phys. Rev. Lett. **92**, 047402 (2004).
[8] S. Leinß, T. Kampfrath, K. v. Volkmann, M. Wolf, J. T. Steiner, M. Kira, S. W. Koch, A. Leitenstorfer, and R. Huber, Phys. Rev. Lett. **101**, 246401 (2008).
[9] F. Junginger, B. Mayer, C. Schmidt, O. Schubert, S. Mährlein, A. Leitenstorfer, R. Huber, and A. Pashkin, Phys. Rev. Lett. **109**, 147403 (2012).
[10] H. Hirori, K. Shinokita, M. Shirai, S. Tani, Y. Kadoya, and K. Tanaka, Nat. Commun. **2**, 594 (2011).
[11] M. Liu, H. Y. Hwang, H. Tao, A. C. Strikwerda, K. Fan, G. R. Keiser, A. J. Sternbach, K. G. West, S. Kittiwatanakul, J. Lu, S. A. Wolf, F. G. Omenetto, X. Zhang, K. A. Nelson, and R. D. Averitt, Nature (London) **487**, 345 (2012).
[12] B. Zaks, R. B. Liu, and M. S. Sherwin, Nature (London) **483**, 580 (2012).
[13] K.-L. Yeh, M. C. Hoffmann, J. Hebling, and K. A. Nelson, Appl. Phys. Lett. **90**, 171121 (2007).
[14] J. Hebling, K.-L. Yeh, M. C. Hoffmann, B. Bartal, and K. A. Nelson, J. Opt. Soc. Am. B **25**, B6 (2008).
[15] H. Hirori, A. Doi, F. Blanchard, and K. Tanaka, Appl. Phys. Lett. **98**, 091106 (2011).
[16] J. R. Danielson, Y.-S. Lee, J. P. Prineas, J. T. Steiner, M. Kira, and S. W. Koch, Phys. Rev. Lett. **99**, 237401 (2007).
[17] H. Hirori, M. Nagai, and K. Tanaka, Phys. Rev. B **81**, 081305(R) (2010).
[18] B. Ewers, N. S. Köster, R. Woscholski, M. Koch, S. Chatterjee, G. Khitrova, H. M. Gibbs, A. C. Klettke, M. Kira, and S. W. Koch, Phys. Rev. B **85**, 075307 (2012).
[19] D. Grischkowsky, S. Keiding, M. v. Exter, and Ch. Fattinger, J. Opt. Soc. Am. B **7**, 2006 (1990).
[20] R. L. Jones and P. Fisher, J. Phys. Chem. Solids **26**, 1125 (1965).
[21] A. Baldereschi and N. O. Lipari, Phys. Rev. B **9**, 1525 (1974).
[22] The field strength inside the sample was evaluated by taking into account Fresnel reflection loss at the sample surface. The Fresnel coefficient for the transmission at the sample surface $t = 2/(n_{\mathrm{Ge}} + 1)$ is 0.41, assuming that the refractive index of germanium in the THz region $n_{\mathrm{Ge}} = \sqrt{\varepsilon_{\mathrm{b}}}$ is 3.9 in Ref. 23.
[23] P. Clauws, J. Broeckx, E. Rotsaert, and J. Vennik, Phys. Rev. B **38**, 12377 (1988).
[24] R. N. Dexter, H. J. Zeiger, and B. Lax, Phys. Rev. **104**, 637 (1956).
[25] D. L. Dexter, Solid State Phys. **6**, 353 (1958).
[26] A. M. Stoneham, *Theory of Defects in Solids* (Clarendon, Oxford, UK, 1975).
[27] K. M. Itoh, J. Muto, W. Walukiewicz, J. W. Beeman, E. E. Haller, H. Kim, A. J. Mayur, M. D. Sciacca, A. K. Ramdas, R. Buczko, J. W. Farmer, and V. I. Ozhogin, Phys. Rev. B **53**, 7797 (1996).
[28] The other fixed parameter is the carrier scattering rate $\gamma/2\pi = 0.1$ THz. In addition, it is assumed that the sum of N_{b} and N_{f} is a constant value, $N_{\mathrm{b}} + N_{\mathrm{f}} = 1.4 \times 10^{15}$ cm^{-3}. Upon increasing $E_{\mathrm{THz\text{-}pump}}$ from 0 to 6 kV/cm, the resonant frequencies $\omega_{1,2}/2\pi$ do not change significantly and are about 2.0 and 2.2 THz, whereas $\gamma_{1,2}/2\pi$ increase from 0.03 to 0.09 THz and from 0.04 to 0.13 THz, maybe because of an increase in the free hole density and scattering rate between impurities and free holes.
[29] P. Janiszewski and M. Suffczynski, Solid State Commun. **37**, 819 (1981).
[30] L. V. Keldysh, Sov. Phys. JETP **20**, 1307 (1965).
[31] The Keldysh parameter K corresponds to the ratio of frequencies between the tunneling and laser field. For the acceptor state of Ge:Ga, K is given by $K = \sqrt{2m^*_{\mathrm{lh}}\omega^2 I_{\mathrm{p}}}/eE_{\mathrm{THz}}$, where the effective mass of the light hole $m^*_{\mathrm{lh}} = 0.043m_0$ is used since the tunneling occurs mainly between the acceptor state and light hole band (Refs. 24 and 36).
[32] τ_{b} for an ionized accepter density N of 1.4×10^{15} cm^{-3} at a temperature T of 15 K can be estimated from $\tau_{\mathrm{b}} = \tau_0(N_0/N)(T/T_0)^{3/2}$ to be ~6 ns (Ref. 34). Here, $\tau_0 = 2.3$ ns is the recombination time for the ionized acceptor density N_0 (=5.2×10^{14} cm^{-3}) at temperature T_0 (=4.2 K) (Ref. 35). This long decay time coupled with the lack of photoexcitation mentioned in the text suggests that not enough holes populate the excited Rydberg states for them to be detected as photothermal-ionized holes.
[33] W. J. Moore and H. Shenker, Infrared Phys. **5**, 99 (1965).
[34] I. S. Park, E. E. Haller, E. N. Grossman, and D. M. Watson, Appl. Opt. **27**, 4143 (1988).
[35] F. A. Hegmann, J. B. Williams, B. Cole, and M. S. Sherwin, Appl. Phys. Lett. **76**, 262 (2000).
[36] H. Q. Nie and D. Coon, Solid State Electron. **27**, 53 (1984).
[37] A. Dargys and S. Zurauskas, J. Phys.: Condens. Matter **7**, 2133 (1995).